

The nuclear matrix elements of 0 decay and the NUMEN project at INFN-LNS

Original

The nuclear matrix elements of 0 decay and the NUMEN project at INFN-LNS / Carbone, D.; Cappuzzello, F.; Agodi, C.; Cavallaro, M.; Acosta, L.; Bonanno, D.; Bongiovanni, D.; Boztosun, I.; Calabrese, S.; Calvo, D.; Chavez Lomeli, E. R.; Delaunay, F.; Deshmukh, N.; Finocchiaro, P.; Fisichella, M.; Foti, A.; Gallo, G.; Hacisalihoglu, A.; Iazzi, F.; Introzzi, R.; Lanzalone, G.; Linares, R.; Longhitano, F.; Lo Presti, D.; Medina, N.; Muoio, A.; Oliveira, J. R. B.; Pakou, A.; Pandola, L.; Pinna, F.; Reito, S.; Russo, G.; Santagati, G.; Sgouros, O.; Solakci, S. O.; Soukeras, V.; Souliotis, G.; Spatafora, A.; Torresi, D.; Tudisco, S.; Yildirim, A.; Zagatto, V. A. B.. - In: EPJ WEB OF CONFERENCES. - ISSN 2101-6275. - 194 (2018), p. 02001. (Intervento presentato al convegno 2018 International Conference on Nuclear Structure and Related Topics, NSRT 2018 tenutosi a bgr nel 2018) [10.1051/epjconf/201819402001].
Availability: This version is available at: 11583/2836216 since: 2024-06-17 11:45:50Z

Publisher:

EDP Sciences

Published

DOI:10.1051/epjconf/201819402001

Terms of use:

This article is made available under terms and conditions as specified in the corresponding bibliographic description in the repository

Publisher copyright

(Article begins on next page)

The nuclear matrix elements of $0\nu\beta\beta$ decay and the NUMEN project at INFN-LNS

D. Carbone^{1,*}, F. Cappuzzello^{1,2}, C. Agodi¹, M. Cavallaro¹, L. Acosta³, D. Bonanno⁴, D. Bongiovanni¹, I. Boztosun⁵, S. Calabrese^{1,2}, D. Calvo⁶, E.R. Chávez Lomelí³, F. Delaunay^{6,7}, N. Deshmukh¹, P. Finocchiaro¹, M. Fisichella⁶, A. Foti⁴, G. Gallo^{1,2}, A. Hacısalihoglu^{1,8}, F. Iazzi^{6,9}, R. Introzzi^{6,9}, G. Lanzalone^{1,10}, R. Linares¹¹, F. Longhitano⁴, D. Lo Presti^{2,4}, N. Medina¹², A. Muoio¹, J.R.B. Oliveira¹², A. Pakou¹³, L. Pandola¹, F. Pinna^{6,9}, S. Reito⁴, G. Russo^{2,4}, G. Santagati¹, O. Sgouros^{1,13}, S.O. Solakci⁵, V. Soukeras^{1,13}, G. Souliotis¹⁴, A. Spatafora^{1,2}, D. Torresi¹, S. Tudisco¹, A. Yildirim⁵, V.A.B. Zagatto¹¹ for the NUMEN collaboration

¹INFN-Laboratori Nazionali del Sud, Catania, Italy

²Università degli Studi di Catania, Catania, Italy

³Universidad Nacional Autónoma de México, Ciudad de México, Mexico

⁴INFN-Sezione di Catania, Catania, Italy

⁵Akdeniz University, Antalya, Turkey

⁶INFN-Sezione di Torino, Turin, Italy

⁷LPC Caen, Normandie Université, ENSICAEN, UNICAEN, CNRS/IN2P3, Caen, France

⁸Istitute of Natural Science, Karadeniz Teknik Universitesi, Trabzon, Turkey

⁹DISAT, Politecnico di Torino, Turin, Italy

¹⁰Università di Enna "Kore", Enna, Italy

¹¹Universidade Federal Fluminense, Niteroi, Brazil

¹²Universidade de Sao Paulo, Sao Paulo, Brazil

¹³University of Ioannina, Ioannina, Greece

¹⁴Laboratory of Physical Chemistry, Department of Chemistry, National and Kapodistrian University of Athens, Athens, Greece

Abstract. The goal of NUMEN project is to access experimentally driven information on Nuclear Matrix Elements (NME) involved in the neutrinoless double beta decay ($0\nu\beta\beta$), by high-accuracy measurements of the cross sections of Heavy Ion (HI) induced Double Charge Exchange (DCE) reactions. The knowledge of the nuclear matrix elements is crucial to infer the neutrino average masses from the possible measurement of the half-life of $0\nu\beta\beta$ decay and to compare experiments on different isotopes. In particular, the (^{18}O , ^{18}Ne) and (^{20}Ne , ^{20}O) reactions are performed as tools for $\beta^+\beta^+$ and $\beta^-\beta^-$ decays, respectively. The experiments are performed at INFN - Laboratory Nazionali del Sud (LNS) in Catania using the Superconducting Cyclotron (CS) to accelerate the beams and the MAGNEX magnetic spectrometer to detect the reaction products. The measured cross sections are very low, limiting the present exploration to few selected isotopes of interest in the context of typically low-yield experimental runs. In order to make feasible a systematic study of all the candidate nuclei, a major upgrade of the LNS facility is foreseen to increase the experimental yield of about two orders of magnitude. To this purpose, frontier technologies are going to be developed for both the accelerator and the detection systems. In parallel, advanced theoretical models will be developed to extract the nuclear structure information from the measured cross sections.

1 Introduction

The neutrinoless double beta ($0\nu\beta\beta$) decay is widely searched in many facilities all over the world because its observation would have fundamental implications. It would establish the Majorana nature of neutrino and has the potential to shed light on the absolute neutrino mass and hierarchy. The $0\nu\beta\beta$ decay basically involves nuclei, thus its analysis necessarily implies nuclear structure ingredients. Indeed, the $0\nu\beta\beta$ decay rate is factorized in three independent factors: the phase-space factor, the Nuclear Matrix Element (NME) and a term that –

assuming a decay mediated by the exchange of Majorana neutrinos – contains the effective neutrino masses. Thus, the precise knowledge of NMEs is necessary to extract information on the neutrino masses, when the decay rate will be possibly measured, and to convert the actual limits on the half-life established by the experiments with different isotopes into limits on the neutrino mass. A comparison between the numerous evaluations of the NME, obtained within various nuclear structure frameworks [1-4], indicates that significant differences are still found, due to ambiguities in the models and the lack of strong constraints. In addition, some assumption

* Corresponding author: carboned@lns.infn.it

common to different competing calculations, like the unavoidable truncation of the nuclear many body wavefunction, could cause overall systematic uncertainties.

In order to obtain experimentally driven information on the NMEs, the NUMEN [5] and the NURE [6-7] projects propose to study Heavy-Ion induced Double Charge Exchange (HIDCE) reactions. These reactions are characterized by the transfer of two charge units, leaving the mass number unchanged, and can proceed by a sequential nucleon transfer mechanism or by meson exchange. Even if $0\nu\beta\beta$ decays and HIDCE reactions are mediated by different interactions, there are a number of similarities among them: the key aspects are that initial and final nuclear states are the same and the transition operators in both cases present a superposition of isospin, spin-isospin and rank-two tensor components with a relevant available momentum (100 MeV/c or so).

The experimental activity of the projects is mainly performed at the INFN-Laboratori Nazionali del Sud (LNS) in Catania using the high-resolution beams accelerated by the Superconducting Cyclotron (CS) and the MAGNEX large acceptance magnetic spectrometer, characterized by high resolution in energy, mass and angle [8-9]. Indeed, the high-order solution of the equation of motion implemented in MAGNEX guarantees high performances and its relevance in the research of heavy-ion physics [10-15], also taking advantage of its coupling to the EDEN neutron detector array [16-17].

We already established the experimental feasibility of HIDCE reactions by studying the $^{40}\text{Ca} (^{18}\text{O}, ^{18}\text{Ne})^{40}\text{Ar}$ reaction at 15 A·MeV with the aim to measure the absolute cross section at zero degree [18]. This pilot experiment demonstrated that high resolution and statistically significant experimental data can be measured for DCE processes and that precious information towards NME determination could be at our reach [18].

Recently, we focused the experimental activity on the nuclei of interest for $0\nu\beta\beta$ decay. In particular, the ($^{20}\text{Ne}, ^{20}\text{O}$) DCE reactions at 15 A·MeV on ^{116}Cd , ^{76}Ge and ^{130}Te , were recently measured for the first time.

2 The project

The aim of the NUMEN project is to measure the absolute cross section for HIDCE reactions on nuclei candidates for the $0\nu\beta\beta$ decay and find a connection between the NMEs of the two processes. The challenge is to isolate and measure a very rare nuclear transition among a very high rate of heavy ions produced by the beam-target interaction. With respect to the pilot experiment, performed on ^{40}Ca target, there are some additional difficulties, which could correspond to an overall reduction of the collected yield:

- a) The Q -value for HIDCE reactions on the nuclei of interest for the $0\nu\beta\beta$ is typically more negative than in the case of ^{40}Ca [18].
- b) The large value of the B(GT) strengths in the ($^{18}\text{O}, ^{18}\text{Ne}$) reaction, which emulate the $\beta^+\beta^+$ decays, makes it particularly advantageous. The ($^{18}\text{Ne}, ^{18}\text{O}$)

reaction, which could be exploited to look at reactions of the $\beta^+\beta^+$ kind, requires a radioactive beam that cannot be available with comparable intensity. The proposed ($^{20}\text{Ne}, ^{20}\text{O}$) has smaller B(GT).

c) The study of some nuclei requires gas or implanted targets, e.g. ^{136}Xe or ^{130}Xe , which are normally much thinner than solid-state ones.

d) In some cases, the achievable energy resolution is not enough to isolate the transition to the ground from the excited states in the final nucleus. Thus, the coincident detection of γ -rays from the de-excitation of the populated excited states is mandatory.

Consequently, the present limits of the facility in terms of beam power (~100 W) for the CS accelerator and acceptable rate for the MAGNEX focal plane detector (few kHz) allow us to concentrate on only few cases, which are planned in the NURE project [6-7] (e.g. ^{116}Cd , ^{130}Te , ^{76}Ge).

The systematic exploration of all the nuclei of interest for $0\nu\beta\beta$ decay, foreseen in the NUMEN project, needs an upgraded set-up able to work at about two orders of magnitude more intense beams [5]. The plan is to:

1. change the beam extraction technology from electrostatic deflector to a stripper foil [19];
2. increase the supplied current of the MAGNEX magnets to reach a higher maximum magnetic rigidity, preserving the geometry and field uniformity of the magnetic fields [20-21] in order to keep the high-precision of the present trajectory reconstruction;
3. install a beam dump to stop the high power beams, keeping the generated radioactivity under control;
4. develop suitable isotopically enriched thin targets to be used in the experiments equipped with a cooling system, which is necessary to dissipate the heat produced by the passage of the intense beam [22];
5. substitute the present MAGNEX Focal Plane Detector gas tracker, based on multiplication wire technology, with a tracker based on micro patterned gas detector [23-24];
6. substitute the wall of silicon pad stopping detectors with SiC detectors [25-26] or similar [27] for the particle identification;
7. introduce an array of detectors for measuring the coincident γ -rays [28];
8. develop suitable front-end and read-out electronics, capable to guarantee a fast read-out of the detector signals, still preserving a high signal to noise ratio [29-30];
9. develop a suitable architecture for data acquisition, storage and data treatment, including accurate detector response simulations.

Finally, the development of a specific theory program to allow an accurate extraction of nuclear structure information from the measured cross sections is part of the NUMEN project. Relying on the use of the DWBA approximation for the cross section, the theoretical activity of the project is focused on the development of microscopic models for DCE reactions, employing several approaches (QRPA, shell model, IBM) for inputs connected to nuclear structure quantities.

3 The experiments

Experimental investigations of the (^{20}Ne , ^{20}O) DCE reaction on ^{116}Cd , ^{76}Ge and ^{130}Te targets were recently performed for the first time. The $^{20}\text{Ne}^{10+}$ beam was accelerated by the INFN-LNS CS at 15 AMeV. Thin solid targets were used, whose thicknesses were carefully chosen in order to guarantee an energy resolution that allows to solve the transition to the residual nucleus ground state from its first excited state. ^{116}Cd rolled target of $1370 \mu\text{g}/\text{cm}^2$ thickness and ^{76}Ge ($386 \mu\text{g}/\text{cm}^2$ thickness) and ^{130}Te ($247 \mu\text{g}/\text{cm}^2$ thickness) both evaporated on a C backing of $\sim 50 \mu\text{g}/\text{cm}^2$ were used. The thickness of ^{116}Cd is much higher than that of ^{76}Ge and ^{130}Te , because the first excited state in the populated ^{116}Sn residual nucleus is at 1.293 MeV, to be compared to 0.559 MeV in ^{76}Se and 0.536 MeV in ^{130}Xe . The MAGNEX spectrometer was placed at forward angles including zero degree in the full acceptance mode ($\sim 50 \text{msr}$).

The study of the (^{20}Ne , ^{20}O) reaction at zero degree implies a peculiar experimental issue. For a measurement that include zero degree, the magnetic fields are set in order to transport the beam ions, $^{20}\text{Ne}^{10+}$ in the present case, towards the faraday cup position at the focal plane. However, when the beam passes through the targets a charge state distribution is originated. At the present experimental conditions, the maximum of the distribution corresponds to the fully stripped $^{20}\text{Ne}^{10+}$ ($\sim 99\%$), but a sizeable amount 9^+ and 8^+ charge states is also present. The magnetic rigidity of these lower charge state components is very close to that of the ejectiles of interest: $^{20}\text{F}^{9+}$ for the Single Charge Exchange (SCE) and $^{20}\text{O}^{8+}$ for DCE. Consequently, they enter in the FPD acceptance causing a limitation in beam intensity tolerable by the detector. It is possible to minimize the amount of $^{20}\text{Ne}^{9+}$ and $^{20}\text{Ne}^{8+}$ beams placing a second target downstream of the primary one to be used as a post-stripper material. After testing many different materials, the final choice was a thick C foil of $\sim 800 \mu\text{g}/\text{cm}^2$. With this configuration the charge state distribution is $\sim 99.1\%$ of 10^+ , $\sim 9.0 \cdot 10^{-3}\%$ of 9^+ and $\sim 2.0 \cdot 10^{-5}\%$ of 8^+ [31]. This solution allowed only a partial reduction of the background and thus a system of shields before the FPD entrance was also equipped to stop such ejectiles.

4 The data reduction

The low cross section of the DCE reaction correspond to a low collected yield for such channel in the experiments performed with the actual INFN-LNS facility. Thus, also the data reduction procedure presents some challenges connected to the identification of heavy ejectiles and the correction of the high-order aberrations through the ray-reconstruction procedure. The identification in terms of atomic number (Z), mass number (A) and charge state (q) is performed according to the technique described in Ref. [32], which provides mass resolution as high as $1/160$. In particular, the atomic number (Z) is identified by the standard ΔE - E technique. A typical ΔE - E

bidimensional plot is shown in Fig. 1 (upper panel) for a single silicon detector together with a coarse graphical contour that includes the Oxygen ejectiles. The plotted parameters are the residual energy measured by the silicon detectors (E_{resid}) in abscissa, and the total energy-loss in the gas part ΔE_{tot} in ordinate.

For the mass identification, a technique that exploits the property of the Lorentz force is adopted. The technique makes use of the relationship between the horizontal position at the focal plane (X_{foc}) and E_{resid} , which is approximately quadratic with a factor depending on the ratio m/q^2 . In a X_{foc} versus E_{resid} plot, as shown in Fig. 1 lower panel for the data selected with the graphical condition on the ΔE_{tot} - E_{resid} one (Fig. 1 upper panel), the ions are distributed on different loci according to the ratio m/q^2 and a clear separation between the different Oxygen isotopes is evident. The selection of the $^{20}\text{O}^{8+}$ ejectiles can be safely performed, as indicated by the graphical contour in the lower panel of Fig. 1.

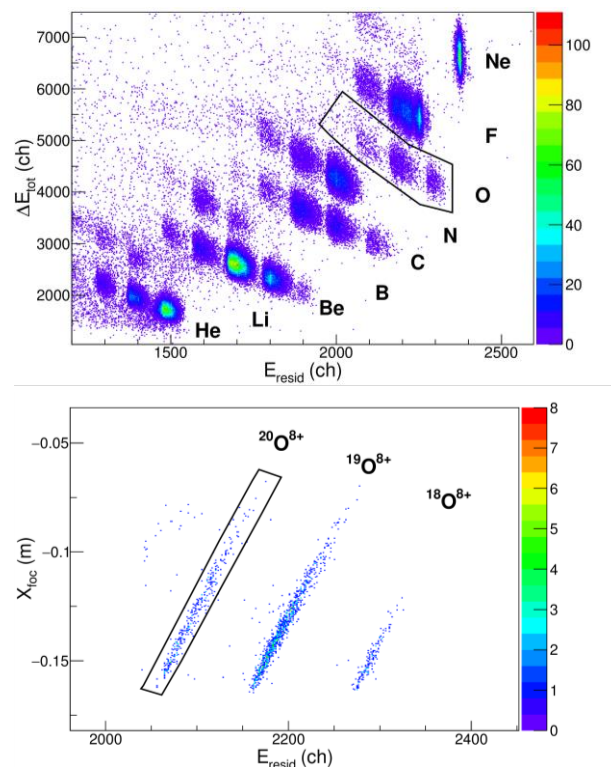


Figure 1. (Upper panel) Typical ΔE_{tot} vs E_{resid} plot for the ejectiles detected in the reaction $^{20}\text{Ne} + ^{116}\text{Cd}$ at 15 MeV/u incident energy for a single silicon detector. The different atomic species and a coarse graphical contour on the oxygen region are indicated. (Lower panel) Typical X_{foc} - E_{resid} plot for the data selected by the graphical condition on the ΔE_{tot} - E_{resid} for the same silicon detector. The different oxygen isotopes and a graphical contour selecting the $^{20}\text{O}^{8+}$ ejectiles are indicated.

The next step of the data reduction is the application of the ray-reconstruction procedure to the identified set of data, according to the Refs. [32, 33]. This allows to extract the momentum vector at the reaction point of the ejectiles and the absolute cross section. A major achievement of the technique is the very small

systematic error obtained in the horizontal θ_i ($-0.01^\circ \pm 0.04^\circ$) and vertical ϕ_i ($-0.05^\circ \pm 0.3^\circ$) angles as well as a high resolution in θ_i (0.2°) and ϕ_i (0.7°) angles [33]. Regarding the reconstructed momentum modulus, a resolution of 1/1800 with an accuracy better than 1/1600 is obtained for the reaction channels of interest.

Despite all the experimental limitations, we are able to measure energy spectra and absolute cross sections for the DCE reaction channel. We measured also other reaction channels (one- and two-proton transfer, one- and two-neutron transfer and SCE), in order to estimate the role of the sequential multi-nucleon transfer routes on the diagonal DCE process. The data reduction and analysis are almost completed and the results will be published soon.

This project has received funding from the European Research Council (ERC) under the European Union's Horizon 2020 research and innovation programme (grant agreement No 714625).

References

1. J. D. Vergados, H. Ejiri and F. Šimkovic, Rep. Prog. Phys. **75**, 106301 (2012)
2. P. Vogel, J. Phys. G: Nucl. Part. Phys. **39**, 124002 (2012)
3. J. Engel and J. Menéndez, J. Rep. Prog. Phys. **80**, 046301 (2017)
4. S. Dell'Oro, S. Marcocci, M. Viel and F. Vissani, Adv. High Energy Phys. **2016**, 2162659F (2016)
5. F. Cappuzzello *et al.*, Eur. Phys. J. A **54**, 72 (2018)
6. M. Cavallaro *et al.*, PoS(BORMIO2017) (2017)
7. M. Cavallaro, PoS(NEUTEL2017) **031** (2017)
8. F. Cappuzzello *et al.*, Eur. Phys. J. A **52**, 167 (2016)
9. F. Cappuzzello *et al.*, Nucl. Instr. Meth. A **763**, 314 (2014)
10. F. Cappuzzello *et al.*, Nature Communications **6**, 6743 (2015)
11. M. Cavallaro *et al.*, Phys. Rev. C **93**, 064323 (2016)
12. D. Carbone *et al.*, Phys. Rev. C **95**, 034603 (2017)
13. J. R. B. Oliveira, J. Phys. G: Nucl. Part. Phys. **40**, 105101 (2013)
14. D. Carbone *et al.*, J. Phys.: Conf. Ser. **312**, 082016 (2011)
15. M. J. Ermamatov, Phys. Rev. C **94**, 024610 (2016)
16. H. Laurent *et al.*, Nucl. Instr. Meth. A **326**, 517 (1993)
17. M. Cavallaro *et al.*, Nucl. Instr. Meth. A **700**, 65 (2013)
18. F. Cappuzzello *et al.*, Eur. Phys. J. A **51**, 145 (2015)
19. L. Calabretta *et al.*, Mod. Phys. Lett. A **32**, 17 (2017)
20. A. Lazzaro *et al.*, Nucl. Instr. Meth. A **585**, 136 (2008)
21. A. Lazzaro *et al.*, Nucl. Instr. Meth. A **602**, 494 (2009)
22. F. Iazzi *et al.*, WIT Transactions on Engineering Sciences **116**, 61 (2017); DOI: 10.2495/MC170071
23. M. Cortesi *et al.*, Review of Scientific Instruments **88**, 013303 (2017)
24. D. Lo Presti *et al.*, J. Phys.: Conf. Series **1056**, 012034 (2018)
25. A. Muoio *et al.*, EPJ Web of Conf. **117**, 10006 (2016)
26. S. Tudisco *et al.*, Sensors **18**, 2289 (2018)
27. D. Carbone *et al.*, Results in Physics **6**, 863 (2016)
28. J. R. B. Oliveira *et al.*, J. Phys.: Conf. Series **1056**, 012040 (2018)
29. D. Bonanno *et al.*, J. Phys.: Conf. Series **1056**, 012006 (2018)
30. D. Bongiovanni *et al.*, J. Phys.: Conf. Series **1056**, 012007 (2018)
31. K. Shima *et al.*, Atom. Data Nucl. Data Tables **51**, 2 (1992)
32. D. Carbone, EPJ. Plus **130**, 143 (2015)
33. F. Cappuzzello *et al.*, Nucl. Instr. Meth. A **638**, 74 (2011)